Texture-Based Algorithm to Separate UWB-Radar Echoes from People in Arbitrary Motion

Takuya Sakamoto, Toru Sato
Graduate School of Informatics
Kyoto University, Kyoto, Japan
Email: t-sakamo@i.kyoto-u.ac.jp

Pascal J. Aubry, and Alexander G. Yarovoy
Microwave Sensing, Signals and Systems
Delft University of Technology, Delft, the Netherlands

Abstract—This study proposes a novel algorithm for separating multiple echoes using texture information of radar images. This algorithm is applied to measurement data to be shown to be effective even in scenarios with motion-varying targets. The performance of the algorithm is investigated through its application to ultra-wide-band radar measurement data for two walking persons.

I. INTRODUCTION

An ultra wide-band (UWB) radar system is a promising sensing tool for indoor navigation because it provides high resolution range and Doppler information. The range information enables the tracking capability of people, whereas the micro-Doppler information is proven to be efficient in estimating the action of each person [1]-[9]. However, these conventional studies all assume that it is a single person in the image data; an effective algorithm is needed for separating multiple targets in the scene.

One such technology is multiple hypothesis tracking (MHT) [10] that employs a Kalman filter and multiple hypothesis technique redesigned for human tracking. Although this technique can estimate multiple trajectories of people, each trajectory is represented as a curve that does not define the actual region corresponding to the target in the radar image. Thus this method does not actually separate the received signals into multiple components so that single-target algorithms can be applied.

In this paper, we propose a new algorithm for separating echoes from multiple persons. This method analyzes the texture of the radar image in the slow time-range domain. The algorithm proposed uses a texture angle that corresponds to a target's line-of-sight speed. Next, we calculate a pixel-connection map in which each pixel is connected to another pixel that has the closest texture angle. Finally, randomly distributed complex values are numerically propagated to the adjacent connected pixels. This algorithm works autonomously even for motion-varying targets. Specifically, we demonstrate that our algorithm can successfully separate echoes from two people walking at different and time-changing speeds.

II. PROPOSED SEPARATION ALGORITHM OF ECHOES

The proposed method consists of three steps. First, we calculate the texture angle of the signal. Second, we obtain a pixel-connection map between pixels of the texture angle image. Third, we apply the connection propagation algorithm to the pixel-connection map to separate multiple echoes.

A. Texture Angle for Radar Echoes

We propose the texture angle for radar images for estimating the approximate line-of-sight velocities of targets. Unlike the use of a spectrogram, the texture angle can estimate the Doppler velocity for each pixel of the image. In general, the echoes of different targets have different texture angles, unless those multiple targets are exactly in the same motion.

We define the texture angle of a slow time-range radar image as

$$\theta(t,r) = \tan^{-1}\left(v_0 \frac{\partial s(t,r)/\partial r}{\partial s(t,r)/\partial t}\right), \qquad (1)$$

where $s(t,r)$ is the signal received at a slow time t from a range r. Note that v_0 is introduced to make the argument of $\tan^{-1}$ dimensionless.

B. Pixel Connection Map based on Texture Angle

Next, we explain the procedure to obtain the pixel-connection map, which corresponds to the second step of our proposed algorithm. In this pixel-connection map, each pixel is connected to another pixel that has the closest texture angle. For this calculation, we use the texture angle of each pixel. Note that the texture angle is defined only if the intensity of the pixel is above a threshold. The following procedure applies only to pixels whose texture angle is defined. For the i-th pixel, the right-connected pixel is chosen as

$$R_i = \arg\min_j |\theta_j - \theta_i|, \qquad (2)$$

subject to

$$t_i + T_s > t_j > t_i \qquad (3)$$

and

$$\left|\tan^{-1}\left(\frac{r_j - r_i}{v_0(t_j - t_i)}\right) - \theta_i\right| < \delta. \qquad (4)$$

Here, T_s is the window size for the search, and δ is a small angle. These conditions imply that the pixel connected to the i-th pixel is located on the right hand side of the i-th pixel, and the inclination of the line connecting the pair of pixels does not contradict the texture angle. Under these conditions, we choose the pixel that has a texture angle closest to that of the pixel of interest.

Similarly, we calculate the left-connected pixels L_i that is located on the left-hand side of the pixel of interest using the same process Eq. (2), but with a different time condition, $t_i - T_s < t_j < t_i$, instead of Eq. (3).

C. Complex Number Propagation Algorithm

Next, we introduce a method that can automatically separate multiple echoes using the pixel connection map R_i and L_i that were calculated in the second step. The pixel connection maps are not entirely accurate; the pixels belonging to different targets can be erroneously connected. The algorithm proposed below benefits from statistical averaging effects to suppress such erroneous connections. This algorithm forms a new image by repetitively updating a few pixels at a time. We call hereafter this image the "connection propagation image", denoted I_n, where $n = 0, 1, \cdots$ is the iteration number.

First, we initialize the connection propagation image I_0. A uniformly distributed random variable $0 \leq \psi < 2\pi$ is chosen independently for each pixel to generate a unit complex number $e^{j\psi}$; if the corresponding amplitude for the pixel is less than the threshold, a zero value is assigned to the pixel of the connection propagation image.

In each iteration, we randomly pick a pixel index $i \in \{1, 2, \cdots, M_p\}$ from the connection propagation image, where M_p is the number of pixels in the connection propagation image. Then the pixels are updated if $t_i \leq (1 + \alpha)T_{\max}/2$ as

$$I_n(t_i, r_i) = (I_{n-1}(t_i, r_i) + I_{n-1}(t_{R_i}, r_{R_i}))/2, \quad (5)$$
$$I_n(t_{L_i}, r_{L_i}) = (I_{n-1}(t_i, r_i) + I_{n-1}(t_{L_i}, r_{L_i}))/2, \quad (6)$$

and updated if $t_i > (1 - \alpha)T_{\max}/2$ as

$$I_n(t_i, r_i) = (I_{n-1}(t_i, r_i) + I_{n-1}(t_{L_i}, r_{L_i}))/2, \quad (7)$$
$$I_n(t_{R_i}, r_{R_i}) = (I_{n-1}(t_i, r_i) + I_{n-1}(t_{R_i}, r_{R_i}))/2, \quad (8)$$

where $T_{\max}$ is the maximum slow-time of the image.

Eqs. (5) and (6) mean that the complex numbers propagate to the left if the chosen pixel is on the left half of the connection propagation image. In contrast, the complex numbers propagate to the right with Eqs. (7) and (8) for pixels on the right half. For i that satisfy $(1 - \alpha)T_{\max}/2 < t_i \leq (1 + \alpha)T_{\max}/2$, all operations Eqs. (5)–(8) are applied, which means that complex numbers propagate in both directions.

In this way, the initialized pixels around the center of the connection propagation image propagate to both sides along the connection established in the previous subsection. Echoes corresponding to different targets have a relatively fewer number of connections, if any. This prevents the complex numbers from being mixed up across adjacent pixels that belong to different targets. After $n = N_{\max}$ iterations, we obtain the final connection propagation image. We use the phase of the connection propagation image $\angle I_{N_{\max}}(t_i, r_i)$ to separate the echoes.

III. Radar Measurement Setup and Data

We measured two persons walking using a PulsOn 400 radar system manufactured by Time Domain Corporation. The frequency band is from 3.1 to 5.3 GHz, and the signal is modulated by an m-sequence. The received data are compressed with the same sequence. The transmitted power is -14.5 dBm. The transmitting and receiving antennas are dual-polarized horn antennas (model DP240 manufactured by Flann Microwave Ltd.) with 2 to 18 GHz bandwidth. The antennas are separated by 50.0 cm.
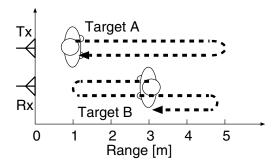

Fig. 1. Schematic of measurement scenario with antennas and two people walking.

Fig. 2. Photo of measurement scenario.

The diagram of the scenario is shown in the lower part of Fig. 1. In this measurement, two persons walked back and forth along the same line. Target A walks from a point 1.0 m away from the antennas to a point 5.0 m away, then back to the original point. Target B walks from a point 3.0 m away from the antennas to a point 1.0 m away, then back to a point 5.0 m away, and walks toward the antenna again. The range measurement repetition frequency is 200 Hz, and the sampling frequency is 16.39 GHz. The received signals are stored and processed afterwards. A photo of the measurement scenario is shown in Fig. 2.

IV. Application of the Proposed Method to Measurement Data

In this section, we apply the set of proposed algorithms to the measurement data: texture angle, the pixel connection map, and the complex number propagation algorithm. For calculating the texture angle, v_0 is set to 1.84 m/s. A 5×5 median filter is applied to the texture angle to eliminate artifacts before calculating a pixel connection map. For the pixel connection map, we set $T_s = 1$ s, and $\delta = 0.1$ rad. For the complex number propagation algorithm, we set $T_h = 0.03 \max |s(t, r)|$, $\alpha = 0.1$, and $T_\theta = \pi/20$.

A slow time-range radar image $|s(t, r)|$ is shown in Fig. 3. The echoes intersect at two points corresponding to 3 s and 10 s. Next, we calculate the texture angle of the slow time-range image (Fig. 4). Each of the two echoes has smooth gradation in the texture angle, which means that speeds of the targets change gradually. This characteristic will be exploited by the proposed method to separate the two echoes.

The proposed pixel-connection map and complex-number propagation algorithm are applied to the texture angle image.
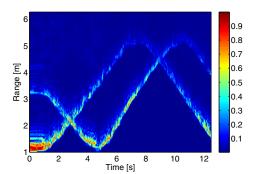
Fig. 3. Slow time-range radar image $|s(t, r)|$ measured for two people walking at time-changing speeds.
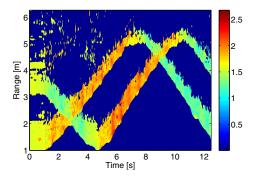

Fig. 4. Texture angle $\theta(t, r)$ calculated, two people walking with time-changing speeds.
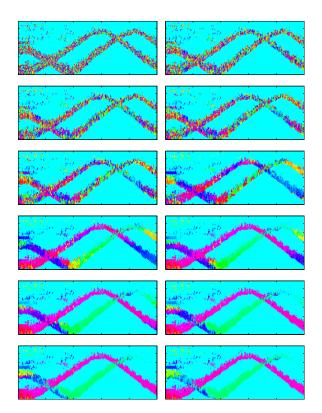

Fig. 5. Iterations in segregating the radar image using the proposed method. The image at the top left is the initialized image. The image at the top right is the image after 2000 iterations. The other images are plotted after 4000, 6000, $\cdots$ iterations (every 2000 iterations).
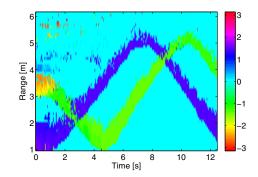
The images in Fig. 5 show the iterative steps of the proposed method, in which the angle of the complex value associated with each pixel is displayed. In the first image, each pixel has an independent value of the others. As the iteration progresses, the dominant colors in the middle of the image propagate toward both sides along the echo trajectories. Even at the intersection points, pixels located nearby each other are not necessarily connected in this algorithm. This is why the colors propagate only to the correctly associated pixels in the image. Finally, most of the pixels in the images are correctly segregated into two dominant colors as seen in the final connection propagation image.

The final connection propagation image after $N_{\max} = 30000$ iterations is shown in Fig. 6. This image indicates that the two targets are clearly separated by our algorithm. A histogram of this image can be used to determine the threshold to separate the two targets. Fig. 7 shows the histogram of the image. We see two significant peaks that correspond to the two targets. In this way, we do not have to know the number of targets in advance to use the proposed method. Multiple echoes are autonomously separated into different colors in this image.

In the same way, even if there are more than two targets, the image can be separated into more than two segments by setting multiple threshold values. To develop a method to find the optimal threshold values for this purpose will be an important aspect of future work. With the proposed algorithm, the signals in the image of Fig. 3 are for the most part clearly separated, as shown in Fig. 8 although some undesired components are seen in the lower image.

Fig. 6. Connection propagation image after applying the proposed method after 30000 iterations (in rad).

V. CONCLUSION

This paper proposes a new algorithm for separating multiple targets using a UWB radar. The proposed method calculates a texture angle to estimate an approximate line-of-sight speed of the target at each pixel of a signal image. Targets with different speeds have different textures in the slow time-range image. The texture angle was combined with other proposed techniques such as the pixel-connection map and the complex number propagation algorithm. The pixel-connection map represents pixels connected by having similar texture angles. A pair of pixels is chosen such that their relative position is in accord with the corresponding pixel of the texture angle image. Finally, randomly distributed complex values are numerically propagated to adjacent connected pixels. This algorithm does
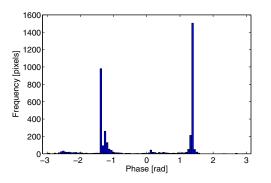
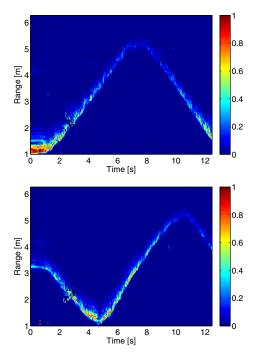Fig. 7. Histogram of the connection propagation image in Fig.6.

Fig. 8. Separated echos $s_1(t, r)$ and $s_2(t, r)$ using the proposed complex number propagation algorithm.

not require a prior knowledge of the number of targets. The randomly assigned complex numbers automatically propagate and merge into multiple segments. We have demonstrated that the proposed algorithm can successfully separate two motion-varying targets from echoes in a measurement with two walking persons.

REFERENCES

[1] Y. Kim and H. Ling, "Human activity classification based on micro-Doppler signatures using a support vector machine," IEEE Transactions on Geoscience and Remote Sensing, vol. 47, no. 5, pp. 1328–1337, May 2009.

[2] A. Sona, R. Ricci and G. Giorgi, "A measurement approach based on micro-Doppler maps for human motion analysis and detection," Proc. IEEE International Instrumentation and Measurement Technology Conference, pp. 354–359, May 2012.

[3] D. Tahmoush and J. Silvious, "Simplified model of dismount micro-Doppler and RCS," Proc. IEEE Radar Conference, pp. 31–34, May 2010.

[4] P. Molchanov, J. Astola and A. Totsky, "Frequency and phase coupling phenomenon in micro-Doppler radar signature of walking human," Proc. 19th International Radar Symposium, pp. 49–53, May 2012.

[5] J. Li, Z. Zeng, J. Sun and F. Liu, "Through-wall detection of human being's movement by UWB radar," IEEE Geoscience and Remote Sensing Letters, vol. 9, no. 6, pp. 1079–1083, Nov. 2012.

[6] C.-P. Lai, R. M. Narayanan, Q. Ruan and A. Davydov, "Hilbert-Huan transform analysis of human activities using through-wall noise and noise-like radar," IET Radar Sonar Navig., vol. 2, no. 4, pp. 244-255, 2008.

[7] A. G. Yarovoy, L. P. Ligthart, J. Matuzas and B. Levitas, "UWB radar for human being detection," IEEE A&E Systems Magazine, pp. 36–40, May 2008.

[8] K. Saho, T. Sakamoto, T. Sato, K. Inoue and T. Fukuda, "Pedestrian classification based on radial velocity features of UWB Doppler radar images" Proc. 2012 International Symposium on Antennas and Propagation, pp. 90–93, 2012.

[9] Y. Wang and A. E. Fathy, "Micro-Doppler signatures for intelligent human gait recognition using a UWB impulse radar," Proc. pp. 2103–2106, 2011.

[10] S.-H. Chang, R. Sharan, M. Wolf, N. Mitsumoto, and J. W. Burdick, "An MHT algorithm for UWB radar-based multiple human target tracking," Proc. IEEE International Conference on Ultra-Wideband, pp. 459–463, Sep. 2009.